Leaf wax and Sr-Nd isotope evidence for high-latitude dust input to the central South China sea and its implication for fertilization

Yang, Yi; Bendle, James A.; Pancost, Richard D.; Yan, Yan; Ruan, Xiaoyan; Warren, Bridget; Lü, Xiaoxia; Li, Xuejie; Yao, Yongjian; Huang, Xianyu; Yang, Huan; Xie, Shucheng

DOI:
10.1029/2020gl091853

Document Version
Peer reviewed version

Citation for published version (Harvard):
Yang, Y, Bendle, JA, Pancost, RD, Yan, Y, Ruan, X, Warren, B, Lü, X, Li, X, Yao, Y, Huang, X, Yang, H & Xie, S 2021, 'Leaf wax and Sr-Nd isotope evidence for high-latitude dust input to the central South China sea and its implication for fertilization', *Geophysical Research Letters*, vol. 48, no. 11, e2020GL091853. https://doi.org/10.1029/2020gl091853

Leaf wax and Sr-Nd isotope evidence for high latitude dust input to the central South China Sea and its implication for fertilization

Yi Yang[1], James A. Bendle[2], Richard D. Pancost[3,4], Yan Yan[5], Xiaoyan Ruan[1], Bridget Warren[2], Xiaoxia Lü[1], Xuejie Li[6], Yongjian Yao[6], Xianyu Huang[1], Huan Yang[1], Shucheng Xie[1,*]

[1] State Key Laboratory of Biogeology and Environmental Geology, School of Earth Sciences, China University of Geosciences, Wuhan 430074, China;

[2] School of Geography, Earth and Environmental Sciences, University of Birmingham, Birmingham, B15 2TT, UK;

[3] Organic Geochemüistry Unit, School of Earth Sciences, School of Chemistry, University of Bristol, Cantock's Close, Bristol BS8 1RJ, UK;

[4] University of Bristol Cabot Institute for the Environment, University of Bristol, Bristol BS8 1UJ;

[5] CAS Key Laboratory of Marginal Sea Geology, Guangzhou Institute of Geochemistry, Chinese Academy of Sciences, Guangzhou, 510640, China;

[6] Guangzhou Marine Geological Survey, Ministry of Land and Resources, Guangzhou 510075, China

*Corresponding author: xiecug@163.com (S. Xie).

Key Points:

1. High concentrations of leaf-wax *n*-alkanes are measured in the South China Sea central basin
2. *n*-Alkane carbon preference index and hydrogen isotopic composition trace aeolian dust deposition from higher latitudes to the central basin
3. Aeolian dust may play a significant role in regulating deposition of terrestrial organic matter in the central South China Sea.

Formatted: Font: Times

Formatted: Font: Times

Abstract

Recent time-series from sediment traps show abnormally high chlorophyll-*a* concentrations and primary productivity in the oligotrophic central South China Sea (SCS), especially during wintertime. Here we present new insights from compound-specific hydrogen isotopic analysis of leaf wax *n*-alkanes and Sr-Nd isotopes extracted from four basin-wide surface sediment transects. We find that the deepest surface sediments in the central basin contain the most depleted *n*-alkane hydrogen isotopes, which is suggestive of inputs from higher latitude soils in northern China. This is further supported by Sr-Nd isotopes of the same surface sediments. We propose that aeolian dust is transported by the winter monsoon and fertilizes the phytoplankton bloom in the central SCS. This process was may have been enhanced during glacial periods due to a stronger winter monsoon, driving both vertical mixing and dust transport to the central basin.

Keywords: *n*-alkane, leaf wax, carbon and hydrogen isotopes, aeolian dust, Sr-Nd isotopes, South China Sea

Plain Language Summary:

Recent studies observe abnormally high winter primary productivity and nitrate concentrations in the surface waters of the central South China Sea. However, this is a nutrient limited region of the ocean, so the drivers of this primary productivity are unclear. Here we analyze leaf wax carbon and hydrogen isotopes, and Sr-Nd isotopes, at four shallow to deep water sediment transects to trace the sources of dust and organic matter in the sediments of the central basin. Our results suggest the central basin sediments receive significant terrestrial inputs of dust and nutrients from northern Asia via long-range aeolian transport (during the winter monsoon). These results give new insights to terrestrial-marine connections and the carbon cycle of the SCS. This process maybe a significant carbon sink in the present-day and during the past.

1. Introduction

The marine biological pump plays an important role in manipulating glacial-interglacial atmospheric CO_2, with the majority of carbon uptake apparently occurring in high latitude oceans such as the Southern Ocean and subarctic Pacific (Brunelle et al., 2010; Martínez-García et al., 2014). Recently, Buchanan et al. (2019) used a global marine biogeochemical model to show that the low latitude ocean could be as important as high latitude locations for regulating atmospheric CO_2 during glacial periods, due to Fe-induced stimulation of dinitrogen (N_2) fixation, strengthening the biological pump, and ultimately causing CO_2 drawdown during glacial periods. This modelling work is consistent with observations from ocean sediments cores that large quantities of sediments enriched in organic carbon are preserved in continental seas and basins along continental margins at low latitudes (Berner, 1982; Hedges and Keil, 1995), suggesting an important role in the global carbon cycle (e.g., Dai et al., 2013; Liu et al., 2010).

The South China Sea (SCS) is the largest marginal sea of the Pacific Ocean. It receives more than 700 million metric tons of fluvial sediments annually from surrounding rivers (Liu and Stattegger, 2014). However, recent evidence highlights anomalously high phytoplankton distributions in the central SCS where fluvial input is usually considered to be insignificant (Ma et al., 2013), indicating the central SCS could be a significant carbon sink (Hung et al., 2020). In particular, satellite observations show phytoplankton blooms, indicated by anomalously high concentrations of Chlorophyll-a, in the central

SCS during winter seasons (Ma et al., 2013; Ma et al., 2019). Export production from phytoplankton blooms contributes a major source of organic matter (OM) to sediments. Sinking particle fluxes including particulate organic matter (POM), calcium carbonate ($CaCO_3$), opal, and lithogenic matter from long-term sediment traps show increased transportation and accumulation of biogenic materials during the winter, within the central basin, compared with northern shallower traps (Li et al., 2017; Ma et al., 2019; Priyadarshani et al., 2019; Zhang et al., 2019). Several 'bottom-up' driving mechanisms of this phenomenon have been proposed, including the intrusion of Kuroshio surface waters (Hung et al., 2007) and mesoscale eddies (Li et al., 2017) during the winter. However, the upwelling events induced by Kuroshio intrusions and meso-scale eddies only account for about 20% of total deposition observed in sediment traps between July 2012 and April 2013 (Zhang et al., 2019). Consequently, modern observations of enhanced winter primary productivity in the central SCS requires an additional mechanism for nutrient delivery.

One such potential driving mechanism is the 'top-down' delivery of dust, loaded with nutrients, from higher latitudes by the East Asian Winter Monsoon (EAWM), which would stimulate nitrogen fixation and the biological pump. Tracers for aeolian dust in marine sediments include minerals (Blank et al., 1985; Liu et al., 2015), chemical components (Mcgee et al., 2016; Uematsu et al., 1983) and terrestrial organics (Bendle et al., 2007; Bendle et al., 2006; Boreddy et al., 2017). Clay minerals and grain sizes as well as chemical components have been discussed as possible input tracers for the SCS (Boulay et al., 2007; Liu et al., 2016), but the mixed signal of the fluvial input, deep water current transportation through Luzon strait, and/or the aeolian dust has made it difficult to confidently appoint the sources of sediments to the central SCS.

The molecular and isotopic composition of leaf wax *n*-alkanes in aerosols has been widely used to evaluate sources and pathways of airborne dust (Bendle et al., 2007; Ohkouchi et al., 1997; Schefuß et al., 2003). For example, the carbon isotopic composition of plant wax *n*-alkanes has been used to map the distribution of C_3/C_4 plants in source regions, and to decipher variations in vegetation in the sediment record throughout the Quaternary (Jia et al., 2012; Li et al., 2015). Moreover, the δ^2H values of modern leaf wax *n*-alkanes are well correlated with the δ^2H of meteoric water at latitudinal scales (Rao et al., 2009) and are increasingly used in palaeohydrological reconstructions (Huang et al., 2018; Thomas et al., 2014). The δ^2H values and carbon preference indices (CPIs; ratio of odd-to-even chained *n*-alkanes) of plant wax *n*-alkanes in East China surface soils exhibit a strong dependence on latitude

and the meteoric δ^2H line (Rao et al., 2009). The SCS region is strongly influenced by the East Asian Monsoon, but whether the δ^2H values of *n*-alkanes from surface sediments can be used to constrain sediment sources in the deep basin, which sits beyond the reach of most fluvial inputs, is still unknown.

We argue that the SCS represents a valuable research opportunity: local fluvial inputs are largely captured on the continental shelf, whilst the middle of central basin (>4000m) sits beyond the reach of most fluvial inputs. Thus, the deep SCS may capture a broad regional signal of aeolian dust inputs (relatively uncontaminated by fluvial or biogenic factors) from a position proximal to the Asian continent. We conduct a basin-wide survey of leaf wax molecular and isotopic distributions and radiogenic Sr-Nd isotopes in the surface sediments of the SCS, and contrast this data with observations and sedimentary of plankton groups in the SCS. This synthesis leads us to infer an increasing biological pump for the anomalous wintertime phytoplankton bloom in the SCS on glacial-interglacial timescales.

2. Samples and Methods

2.1 Sampling sites

A total of 62 surface sediment samples were collected from the SCS (Fig. 1), with water depths ranging from 30 to 4405m. The sampling transect therefore allows a comparison of the preservation of terrestrial organic matter between shallow and deep-water sediments. The samples were collected using a deep-sea sediment grab sampler or a box corer (0-5cm) and stored at -20°C prior to analysis.

2.2 TOC and Sr-Nd isotopic compositions analysis

For the TOC analysis, 1 gram sediment was decalcified with 2M HCl at room temperature for 24h, then rinsed with pure water until pH = 7. Samples were freeze dried and transferred into tin capsules, then analyzed by Elemental Analyzer. For the Sr-Nd isotopes analysis, 20 samples were digested in Teflon bombs with mixed agents of double distilled HNO_3 and HF acid at 190 °C for 48h. Then, samples were detected using a Triton T1 thermal ionization mass spectrometer (TIMS) and a Neptune Plus multi-collector ICP-MS. The measured $^{143}N/^{144}Nd$ and $^{87}Sr/^{86}Sr$ ratios were normalized to $^{146}Nd/^{144}Nd$ = 0.7219 and $^{86}Sr/^{88}Sr$ = 0.1194, respectively. During the analysis, BCR-2 standard gave $^{87}Sr/^{86}Sr$= 0.704989 ± 8 (2σ) and $^{143}N/^{144}Nd$=0.512644 ± 2 (2σ). Nd results are calculated as εNd(0) = [(($^{143}N/^{144}Nd$)/0.512638)-1] × 10000, using the chondritic uniform reservoir value given by Jacobsen and Wasserburg (1980).

2.3 Lipid extraction and analysis.

Samples were freeze dried and homogenized with a pestle and mortar, then subjected to a methodology modified from Yang et al. (2014). Samples were ultrasonically extracted with an azeotrope of dichloromethane: MeOH (v/v 9:1) 5 times. All extracts were combined and collected after centrifugation. The combined extracts were concentrated to 1-2 mL using rotary evaporation and dried under a flow of N_2 gas. The total lipid extract was fractionated with *n*-hexane and MeOH into an apolar fraction (containing the *n*-alkanes) and a polar fraction.

n-Alkanes were detected and identified by an Agilent 7890 gas chromatograph and 5975A mass spectrometer (GC-MS) equipped with a DB-5MS capillary column (60m × 0.25mm × 0.25μm). The alkane fraction was injected at a programmed temperature ramp of 3 °C/min^{-1} from 70 to 300 °C and held at 300 °C for 30 min. Relative compound abundances were calculated by comparing corresponding MS (TIC) peak areas with internal standards of known concentration. Stable carbon and hydrogen isotope compositions of individual *n*-alkanes were determined followed the program of Huang et al. (2014) using a Finnigan Trace GC instrument attached to a Finnigan Delta Plus XP isotope ratio mass spectrometer. Duplicate analyses were used to confirm that the standard deviations of leaf wax carbon and hydrogen isotope determinations were better than ± 0.5‰ and 5‰ respectively. The $\delta^{13}C$ and $\delta^{2}H$ values are reported in the delta notation (‰) relative to Vienna Pee Dee Belemnite (VPDB) and Vienna Standard Mean Ocean Water (VSMOW), respectively.

3. Results

3.1 TOC and Sr-Nd isotope compositions

TOC values range from 0.12% to 0.82% (average 0.43%) in the SCS, and C/N values vary from 1.8 to 8.7 (average 6.3). Both TOC and C/N decrease with distance offshore, with high values in the northern SCS, representing the higher organic matter deposits from fluvial inputs. However, in the central basin, the TOC and C/N show an increase, with values comparable to those of the northern SCS (Fig. 2A), suggesting a distinct source of terrestrial organic matter.

The $^{87}Sr/^{86}Sr$ and $^{143}Nd/^{144}Nd$ ratios range from 0.709161 to 0.712215 (average 0.712125) and from 0.512058 to 0.512425 (average 0.512154), respectively. εNd(0) values range from -11.31 to -4.15 (average -9.45). These values are consistent with previously published data of surface sediments from

160 the SCS (Liu et al., 2015, and references therein). Three samples from the northern and eastern SCS
161 with the highest εNd(0) (-6 to -4) derived from Luzon island (Liu et al., 2015).
162 3.2 Leaf wax molecular and isotopes distributions
163 The surface sediments contain *n*-alkanes characterized by a high odd-over-even carbon number
164 ranging in carbon number from C_{16} to C_{35}, with C_{31} dominant (Fig. S1). This is a clear signature of
165 terrestrial higher plant origin (Bush and McInerney, 2013; Eglinton and Hamilton, 1967). The
166 concentrations of total long chain *n*-alkanes show large variations, with anomalously high
167 concentrations in the deep central basin (Fig. 2B). CPI is typically around 2 in shallow surface sediments,
168 but it increases abruptly to 8 in the deepest basin (Fig. 2C). Concentrations of long chain diols (LCDs)
169 (algal biomarkers) range from 0.1 to 32.7 mg/g TOC dry sediments (Fig. 2D; Yang et al., 2020). It is
170 notable that both *n*-alkanes and planktonic LCDs comprise an enhanced proportion of the total organic
171 carbon (TOC) in the surface sediments deposited in the central basin, with TOC-normalized
172 concentrations up to three orders of magnitude higher in deep sediments than in shallow sediments (Fig.
173 3A-B).
174 Our *n*-alkane $\delta^{13}C$ values shift from -29 to -31‰ from the northeastern coast to the central basin
175 (Fig. 2E-F). The values in the deep central basin are similar to the northern SCS, and are highly variable
176 (Fig. 3E). *n*-Alkane $\delta^{2}H$ values vary from -140 to -160‰ in the northern SCS (Fig. 2G-H), but are
177 depleted in the deep central basin, with minimum values around -200‰. The lowest values (-190 to -
178 200 ‰) are distinct from the values observed in both Southern China catchment soils and the shallow
179 sediments (Fig. 1, Pelejero et al., 2003; Rao et al., 2009).
180
181 **4. Discussion**
182 4.1 Sources of surface sediments in the central SCS
183 The Sr-Nd isotopes from SCS surface sediments and surrounding fluvial drainage systems have
184 been well studied and were used to identify the sediment source provinces (Liu et al., 2016 and
185 references therein). Three samples from the northern and eastern SCS have a more positive εNd(0)
186 falling within the variation range of the Luzon island (Liu et al., 2016), indicating the possible influence
187 of northern Luzon Arc material. The surrounding fluvial inputs have higher values of $^{87}Sr/^{86}Sr$ (>7.2,
188 Liu et al., 2016), which are distinguishable from our deep-water sediments, except for two samples
189 from the Red River. However, the clay mineral assemblages showed limited influence of the Red River

Commented [YY1]: 这后面部分想要去阐述吕宋岛弧和河流输入与深海盆之间的差异

on the SCS central basin (Liu et al., 2016). Our data shows that the more positive εNd(0) and lower $^{87}Sr/^{86}Sr$ isotopes from the central basin sediments are not consistent with, and thus may not originate from the surrounding fluvial drainage systems.

Instead, the $^{87}Sr/^{86}Sr$ and εNd(0) isotopes from the central basin are consistent with Asian dust regions, suggesting a source relationship (Fig. 4A). This result is in line with the geochemical analyses of sediments from Yongxing island in the SCS, which received significant high-latitude Asian aeolian dust inputs (Liu et al., 2014). Grain size of the sediments might exert an impact on the Sr-Nd isotopes as the Sr isotopic compositions are known to be strongly affected by the weathering, transportation and deposition (Chen et al., 2007). The grain size of the sediments ranges from 0-400 μm (average medium diameter >5 μm) in the northern and eastern SCS, but from 0-40 μm (average medium diameter ~ 3μm) in the central SCS basin. Comparison of the grain size fractions suggests the Asian dust (<5 μm) falling in the range of the SCS central basin is mainly contributed by the isotopic region B (i.e, the northern margin of Tibetan Plateau) and C (i.e., the Ordos Plateau) (Fig. 4B). A calculation based on a simple mass balance suggests 1:4 for the relative contribution of the isotopic regions B and C to the SCS central basin (Fig. 4B).

n-Alkane CPIs of ~2 are consistent with those previously observed in shallow sediments from the northern SCS (about 1.4 to 2.9 from Xu et al., 2014), and somewhat lower than those from surrounding surface soils in Southern China (ca. 4, Rao et al., 2009; Luo et al., 2012), as well as northern SCS Holocene sediments (ca. 2.3, Pelejero, 2003). Lower CPIs in marine sediments than in source catchment soils suggest microbial degradation during riverine transportation (Ganeshram et al., 2011; Sun et al., 2005). However, in the deepest SCS sediments, CPIs >3 are observed (Fig. 3C), with the highest CPI measured approaching 8. Such high values are not observed in any of the shallow water settings (Pelejero, 2003; Xu et al., 2014), suggesting that the terrestrial organic matter observed in this deep basin setting is unlikely to be of riverine origin. CPIs of surface soils in eastern and northern China show a strong relationship with latitude, with elevated values (> 5) observed in higher latitudes (Rao et al., 2009). This high latitude CPI signature transported from the Asian dust area is also observed in the deep-sea surface sediments collected from the Central Pacific (Ohkouchi et al., 1997). Comparison of CPI values from SCS surface sediments with latitudinal soil profiles (Fig. S2), highlights that the high CPI values (ca. 8) in the deep basin match source locations at mid-high latitudes (about 40 °N) (Fig. 4C), where the loess plateau (with average CPI at 12.3; Liu and Huang, 2005; Luo et al., 2012) and

Gobi desert are located. Although *n*-alkane CPI covaries with various different environmental factors (latitude, aridity and vegetation types) globally (Luo et al., 2012), latitude is still significant and correlates broadly with CPI values (Fig. S2), with higher CPI in high latitudes. We propose the distinctive CPI signature of the deepest SCS records are related to enhanced terrestrial organic matter contributions via aeolian dust transported directly from vegetation or soils (Chikaraishi and Naraoka, 2003; Ning et al., 2005).

n-Alkane δ^2H values in East China surface soils also exhibit a strong dependence on latitude, with lower values occurring at higher latitudes (Fig. 4D) (Rao et al., 2009). The δ^2H of southern Chinese surface soils are around -160‰, consistent with northern SCS surface sediment values. However, the δ^2H values in the central basin are more depleted and closer to higher latitude soil values (according to the linear correlation between δ^2H and latitude (Fig. 4D)), supporting the above suggestion that *n*-alkanes deposited in the central SCS are sourced from high-latitude dust inputs. The trend with water depth for *n*-alkane $\delta^{13}C$ values in the SCS is more variable than for δ^2H. *n*-Alkane $\delta^{13}C$ is used to trace the relative contribution of C_3 and C_4 plant types. The *n*-alkane $\delta^{13}C$ through the SCS thus likely records the C_3/C_4 plant signal in terrestrial inputs to the SCS. The *n*-alkane $\delta^{13}C$ in the SCS surface sediments is consistent with inputs from a diverse and mixed distribution of C_3 and C_4 plants extending from Southeast Asia throughout mainland China (Still et al., 2009). Thus in this context $\delta^{13}C$ values are not as diagnostic as the corresponding δ^2H values and CPIs for indicative of source regions.

Comparison of *n*-alkane δ^2H and CPI data from the central basin with the available soil *n*-alkane data (this study and Rao et al., 2009, Fig. 4C-D), suggests significant soil inputs from >40 °N, ca. 2000km to the north of the SCS region. High latitude arid and semi-arid regions in China and Asia, especially the Taklimakan desert (located at ca. 35 to 45 °N), are major sources of atmospheric dust in the Northern Hemisphere (add ref). During the winter monsoon, decreased winter precipitation allows more aeolian dust transport to the SCS, while only minimal inputs of entrained dust occurs during the summer monsoon, due to heavy summer precipitation and rainout of dust closer to source regions (Boulay et al., 2003; Tian et al., 2005). We conducted a seasonal back trajectory air masses model which simulated the seasonal organic matter transport pathway to the central SCS (13°N, 115°E). The result shows a larger amount of dust transport from central Asia during the winter season compared to the summer season (Fig. S3), which is consistent with the results from Yongxin island (Xiao et al., 2017). Our *n*-alkane isotopic signatures (low δ^2H values) are consistent with enhanced delivery of aeolian dust

Formatted: Font color: Red

to the central SCS by the winter monsoon. The lipid profile results agree with the $^{87}Sr/^{86}Sr$ and εNd(0) evidence, both confirm dust inputs from high latitude Asian source regions to the deep central basin of the SCS.

4.2 Enhanced Aeolian dust input to the SCS central basin and its implications

Our results show both terrestrial leaf wax *n*-alkane and LCD concentrations increase in the central basin compared to northern SCS. Trace metal (Sr-Nd) isotopes from the same stations also constrain the original sources to predominantly mid-latitude Asian deserts (Fig. 4A-B). It is interesting to note that time-series sediment trap data from the SCS quantified the effects of the different processes on sinking particle fluxes, and highlighted that the northeast winter monsoon and associated aerosol deposition events played key roles in sediment deposition during the winter monsoon period (58.7%, Zhang et al., 2019, from October to April). Consequently, our investigations on surface sediments - and the reported time-series trap data - both indicate an important contribution of Asian dust to the SCS central basin.

Of significance is that Asian dust inputs are elevated during the winter season due to the occurrence of the enhanced Winter Asian Winter Monsoon. This is of importance for connections to the carbon-cycle, via processes such as fertilization of phytoplankton and the rapid deposition of organic matter. Both *n*-alkane and LCD concentrations are elevated in the surface sediments of the central basin compared with the northern SCS, and high *n*-alkane CPI values indicate relatively fresh organic matter deposition to the deepest water sites in the central SCS. These results are consistent with enhanced satellite Chl-a concentration and organic matter collected from time-series sediment traps in the central basin (Li et al., 2017; Ma et al., 2019; Priyadarshani et al., 2019; Zhang et al., 2019). Seasonal time-series data analysis shows higher OM deposition during the winter season when EAWM conditions prevail.

A “bottom-up” mechanism driving phytoplankton blooms and biomass in the marginal, stratified regions of the SCS has been well characterised (Chen, 2005; Tang et al., 1999; Li et al., 2017). During the winter season, the frequency of cold meso-scale eddies increases in the central SCS, which drives nutrient-rich subsurface waters to the surface and stimulates phytoplankton blooms in the oligotrophic SCS central basin (Chen, 2005; Tang et al., 1999). Coupled with the meso-scale eddies during winter season, vertical mixing in the upper water column is strongest in the central basin, and is about four

times deeper in winter than is seen in the rest of the year (Lu et al., 2020; Qu, 2001). Increased vertical mixing drives higher concentrations of nitrate to the surface layer and fertilizes the phytoplankton bloom in the central basin. This mechanism explains the higher nitrate concentration and primary production in the central basin compared to the northern SCS observed in satellite data. Logically, increased carbon export to the SCS during the winter monsoon will lead to the deposition of an outsized proportion of these sediments during that time interval. This bottom-up mechanism successfully explains the abnormal high chl-a and high OC fluxes at the central basin, but cannot reconcile the high terrestrial sourced *n*-alkane distribution in the central SCS.

High concentrations of high CPI *n*-alkanes which are depleted in δ^2H demonstrate the importance of aeolian dust deposition in the transport of organic matter to the central SCS (Fig. 4C-D). We propose a "top-down" mechanism could be essential to explain the observed distributions of *n*-alkane and long chain diols in the surface sediments of the central SCS basin. Windborne dust particles containing both lithogenic material and land-derived lipids are significant in the rapid transfer of newly fixed organic carbon from the sea surface to the bottom (Ittekkot et al., 1992). The incorporation of minerals into biologically formed aggregates ensures the rapid deposition of fresh *n*-alkanes with higher CPI in the central basin. Meanwhile, modern observation studies suggest Asian dust events could enhance phytoplankton growth and primary production in Chinese marginal seas (Tan et al., 2011; Tan et al., 2012; Wang et al., 2012), which further supports evidence from TOC, carbonate, microfossil and lipid profiles studies (Thunell et al., 1992; Huang et al., 1997a; Huang et al., 1997b; Shiau et al., 2008; Ren et al., 2017). Long time *in situ* studies revealed aerosol deposition of dissolved inorganic nitrogen to the SCS, especially in the basin area, was approximately 20% on average (Kim et al., 2014; Shen et al., 2020; Gao et al., 2020). This atmospheric N deposition could support the primary production in the oligotrophic water of the SCS, which is characterized by limited nitrate.

Dust regulated iron supply might stimulate the nitrogen fixation, and is crucial in linking the biological cycling of iron to the assimilation of major nutrients and carbon fixation (Tagliabue et al., 2017). A recent model study shows Fe-induced stimulation of N_2 fixation pathways could drive a considerable uptake of carbon dioxide in low latitude oceans during dusty glacial conditions (Buchanan et al., 2019). Gaye et al. (2009) proposed the N_2 fixation contributed up to 20% to settling particle nitrogen in the deep SCS, about twice the estimated contribution in the northern SCS (Kao et al., 2012; Wong et al., 2007; Zhang et al., 2015). However, both foraminifera-bound nitrogen isotope records and

Formatted: Font: Italic

Commented [MOU2]: Which basin?

Commented [MOU3]: 20% of what? 20% of total annual flux?

ammonia oxidizing archaea records from the SCS (Ren et al., 2017; Dong et al., 2019) reconstruct lower N_2 fixation rates during glacial periods, despite the observed increase in dust deposition and productivity. Thus the role of Fe fertilization in regulating the SCS carbon and nitrogen cycles requires further investigation.

In summary our evidence from terrestrial leaf wax (*n*-alkane) and marine phytoplankton (LCDs) biomarkers is consistent with sediment trap time-series data (ref) and suggests a role for aerosol dust deposition in the winter phytoplankton blooms as observed by satellite in the central basin of the SCS (Ma et al., 2013). During the winter monsoon it appears that dust supplied from higher latitudes and vertical oceanic mixing supplies higher nutrients and triggers new production in the central SCS. Our results are also important for paleoclimate reconstructions, as this process would be expected to deliver enhanced supplies of terrestrial, nutrient baring, dust during the glacial periods (Shiau et al., 2008; Ren et al., 2017). However, precise mechanisms and the relative importance of, for example, Fe fertilization in currently ambiguous. Thus more work, including *in-situ* monitoring in the central basin and model simulations are required to elucidate mechanisms, quantify fluxes and understand the importance of dust deposition at the air-water interface in low latitude marginal seas.

5. Conclusions

Multiple lines of evidence based on high *n*-alkane CPI, depleted δ^2H, and Sr-Nd isotope values in surface sediments highlight the transport and deposition of dust from high latitude regions to the central SCS basin. We conclude aeolian dust from northern China is transported by the East Asia Winter Monsoon and contributes (along with vertical mixing of nutrients) to the triggering of the winter phytoplankton in the central SCS. The intimate biotic-abiotic association trigged by dust supply could accelerate the organic deposition rate and thus has implications for the biological pump. Our results shows that nitrogen fixation in the marginal SCS central basin could be as important as vertical mixing, both in increasing primary production and for high sediment deposition rates. Thus the SCS central basin could be a significant, but hitherto overlooked, carbon sink during the present day and glacial periods, which merits further investigation.

Formatted: Font: Italic

Formatted: Font: Italic

Acknowledgements

We thank the Editors Dr. Angelicque White, Dr. Sarah Feakins and two anonymous reviewers for their constructive comment to improve the quality of this manuscript. The work was supported by the State Key R&D Program of China (Grant No.2016YFA0601100), the National Natural Science Foundation of China (Grant No. 41821001 and 41830319), Guangzhou Marine Geological Survey (Grant No. [2015] GZH01-02-6). We thank the China Scholarship Council (CSC) (Grant No. xxxxx) for supporting Yang Yi's study visit to the University of Birmingham

Formatted: Highlight

Formatted: Highlight

Formatted: Highlight

Data Availability Statement

All of the original data has been uploaded as supplemental material and will be deposited publicly to the repository of Zenodo, once it is accepted for publishing. All the supporting data can be found in the cited references (Rao et al., 2009; Luo et al., 2012; Liu et al., 2007; Pettke et al., 2000; Defant et al., 1990; Jiang et al., 2013; Chen et al., 2007; Liu et al., 2014; Biscaye et al., 1997).

References

Bendle, J., Kawamura, K., Yamazaki, K., Niwai, T. (2007). Latitudinal distribution of terrestrial lipid biomarkers and n -alkane compound-specific stable carbon isotope ratios in the atmosphere over the western Pacific and Southern Ocean. *Geochimica et Cosmochimica Acta*, 71, 5934-5955.

Bendle, J.A., Kawamura, K., Yamazaki, K. (2006). Seasonal changes in stable carbon isotopic composition of n -alkanes in the marine aerosols from the western North Pacific: Implications for the source and atmospheric transport. *Geochimica et Cosmochimica Acta,* 70, 13-26.

Berner, R.A., (1982). Burial of organic carbon and pyrite sulfur in the modern ocean: its geochemical and environmental significance. *America Journal of Science*, 282, 451-473.

Biscaye, P. E., Grousset, F. E., Revel, M., Van der Gaast, S., Zielinski, G. A., Vaars, A., Kukla, G. (1997). Asian provenance of glacial dust (stage 2) in the Greenland Ice Sheet Project 2 ice core, Summit, Greenland. Journal of Geophysical Research: Oceans, 102, 26765-26781.Blank, M., Leinen, M., Prospero, J.M. (1985). Major Asian aeolian inputs indicated by the mineralogy of aerosols and sediments in the western North Pacific. *Nature*, 314, 84-86.

Boreddy, S.K.R., Haque, M.M., Kawamura, K. (2017). Long-term (2001–2012) trends of carbonaceous aerosols

from remote island in the western North Pacific: an outflow region of Asian pollutants and dust. *Atmospheric Chemistry & Physics*, 1-21.

Boulay, S., Colin, C., Trentesaux, A., Clain, S., Liu, Z., Lauer-Leredde, C. (2007). Sedimentary responses to the Pleistocene climatic variations recorded in the South China Sea. *Quaternary Research*, 68, 162-172.

Boulay, S., Colin, C., Trentesaux, A., Pluquet, F., Bertaux, J., Blamart, D., Buehring, C., Wang, P. (2003). Mineralogy and sedimentology of Pleistocene sediment in the South China Sea (ODP Site 1144), Proceedings of the ocean drilling program, scientific results, 1-21.

Brunelle, B.G., Sigman, D.M., Jaccard, S.L., Keigwin, L.D., Plessen, B., Schettler, G., Cook, M.S., Haug, G.H. (2010). Glacial/interglacial changes in nutrient supply and stratification in the western subarctic North Pacific since the penultimate glacial maximum. *Quaternary Science Reviews*, 29, 2579-2590.

Buchanan, P.J., Chase, Z., Matear, R.J., Phipps, S.J., Bindoff, N.L. (2019). Marine nitrogen fixers mediate a low latitude pathway for atmospheric CO2 drawdown. *Nature communications*, 10, 1-10.

Bush, R.T., McInerney, F.A. (2013). Leaf wax *n*-alkane distributions in and across modern plants: implications for paleoecology and chemotaxonomy. *Geochimica et Cosmochimica Acta*, 117, 161-179.

Chen, J., Li, G., Yang, J., Rao, W., Lu, H., Balsam, W., Sun, Y., Ji, J. (2007). Nd and Sr isotopic characteristics of Chinese deserts: implications for the provenances of Asian dust. *Geochimica et Cosmochimica Acta*, 71, 3904-3914.

Chen, Y.-l.L., (2005). Spatial and seasonal variations of nitrate-based new production and primary production in the South China Sea. *Deep Sea Research Part I: Oceanographic Research Papers*, 52, 319-340.

Chikaraishi, Y., Naraoka, H. (2003). Compound-specific $\delta^{13}C$ analyses of *n*-alkanes extracted from terrestrial and aquatic plants. *Phytochemistry*, 63, 361-371.

Dai, M., Cao, Z., Guo, X., Zhai, W., Liu, Z., Yin, Z., Xu, Y., Gan, J., Hu, J., Du, C. (2013). Why are some marginal seas sources of atmospheric CO2? *Geophysical Research Letters*, 40, 2154-2158.

Dong, Liang, Zhiyang Li, and Guodong Jia, (2019). Archaeal ammonia oxidation plays a part in late Quaternary nitrogen cycling in the South China Sea." *Earth and Planetary Science Letters,* 509, 38-46.

Defant, M.J., Maury, R.C., Joron, J.-L., Feigenson, M.D., Leterrier, J., Bellon, H., Jacques, D., Richard, M. (1990). The geochemistry and tectonic setting of the northern section of the Luzon arc (the Philippines and Taiwan). *Tectonophysics*, 183, 187-205.

Eglinton, G., Hamilton, R.J. (1967). Leaf epicuticular waxes. *Science*, 156, 1322-1335.

Ganeshram, R.S., Bryant, C.L., Cisneros, L.M. (2011). Sources of *n*-alkanes in an urbanized estuary: Insights

399 from molecular distributions and compound-specific stable and radiocarbon isotopes. *Marine Chemistry*, 126,
400 239-249.
401 Gao, Y., Wang, L., Guo, X., Xu, Y. and Luo, L., (2020). Atmospheric wet and dry deposition of dissolved inorganic
402 nitrogen to the South China Sea. *Science China Earth Sciences*, *63*(9), 1339-1352.
403 Gaye, B., Wiesner, M., Lahajnar, N. (2009). Nitrogen sources in the South China Sea, as discerned from stable
404 nitrogen isotopic ratios in rivers, sinking particles, and sediments. *Marine Chemistry* 114, 72-85.
405 Hedges, J.I., Keil, R.G. (1995). Sedimentary organic matter preservation: an assessment and speculative synthesis.
406 *Marine Chemistry*, 49, 81-115.
407 Huang, C. Y., P. M. Liew, M. Zhao, T. C. Chang, C. M. Kuo, M. T. Chen, C. H. Wang, and L. F. Zheng, (1997a):
408 Deep sea and lake records of the Southeast Asian paleomonsoons for the last 25 kyrs. *Earth and Planetary Science*
409 *Letters*, 146, 59-72.
410 Huang, C. Y., S. F. Wu, M. Zhao, M. T. Chen, C. H. Wang, X. Tu, and P. B. Yuan, (1997b): Surface ocean and
411 monsoon climate variability in the South China Sea since last glaciation. *Marine Micropaleontology,* **32**, 71-
412 94.Huang, X., Pancost, R.D., Xue, J., Gu, Y., Evershed, R.P., Xie, S., (2018). Response of carbon cycle to drier
413 conditions in the mid-Holocene in central China. *Nature communications*, 9, 1-9
414 Huang, X., Xue, J., Meyers, P.A., Gong, L., Wang, X., Liu, Q., Qin, Y., Wang, H. (2014). Hydrologic influence
415 on the δ13C variation in long chain n -alkanes in the Dajiuhu peatland, central China. *Organic Geochemistry*,
416 69, 114-119.
417 Hung, J.-J., Wang, S.-M., Chen, Y.-L. (2007). Biogeochemical controls on distributions and fluxes of dissolved
418 and particulate organic carbon in the Northern South China Sea. *Deep Sea Research Part II: Topical Studies*
419 *in Oceanography*, 54, 1486-1503.
420 Hung, J.-J., Wang, Y.-J., Tseng, C.-M., Chen, Y.-L.L. (2020). Controlling mechanisms and cross linkages of
421 ecosystem metabolism and atmospheric CO2 flux in the northern South China Sea. *Deep Sea Research Part*
422 *I: Oceanographic Research Papers*, 157, 103205.
423 Ittekkot, V., Haake, B., Bartsch, M., Nair, R.R. and Ramaswamy, V., (1992). Organic carbon removal in the sea:
424 the continental connection. *Geological Society, London, Special Publications*, 64(1), 167-176.
425 Jacobsen, S.B., Wasserburg, G. (1980). Sm-Nd isotopic evolution of chondrites. *Earth and Planetary Science*
426 *Letters*, 50, 139-155.
427 Jia, G., Li, Z., Peng, P.A., Zhou, L. (2012). Aeolian n -alkane isotopic evidence from North Pacific for a Late
428 Miocene decline of C4 plant in the arid Asian interior. *Earth and Planetary Science Letters*, 321, 32-40.

Jiang, F., Frank, M., Li, T., Chen, T.Y., Xu, Z., Li, A. (2013). Asian dust input in the western Philippine Sea: Evidence from radiogenic Sr and Nd isotopes. *Geochemistry, Geophysics, Geosystems*, 14, 1538-1551.

Kao, S.J., Terence Yang, J.Y., Liu, K.K., Dai, M., Chou, W.C., Lin, H.L., Ren, H. (2012). Isotope constraints on particulate nitrogen source and dynamics in the upper water column of the oligotrophic South China Sea. *Global biogeochemical cycles*, 26,1-15.

Kim, T. W., Lee,K., Duce,R., Liss,P. (2014). Impact of atmospheric nitrogen deposition on phytoplankton productivity in the South China Sea, *Geophysical Research Letters*, 41, 3156-3162.

Li, H., Wiesner, M.G., Chen, J., Ling, Z., Zhang, J., Ran, L. (2017). Long-term variation of mesopelagic biogenic flux in the central South China Sea: Impact of monsoonal seasonality and mesoscale eddy. *Deep Sea Research Part I: Oceanographic Research Papers*, 126, 62-72.

Li, L., Li, Q., Li, J., Wang, H., Dong, L., Huang, Y., Wang, P. (2015). A hydroclimate regime shift around 270 ka in the western tropical Pacific inferred from a late Quaternary n -alkane chain-length record. *Palaeogeography Palaeoclimatology Palaeoecology*, 427, 79-88.

Liu, K.-K., Atkinson, L., Quiñones, R., Talaue-McManus, L. (2010). Carbon and nutrient fluxes in continental margins: a global synthesis. Springer Science & Business Media.

Liu, Q., Sun, Y., Qiang, X., Tada, R., Hu, P., Duan, Z., Jiang, Z., Liu, J., Su, K. (2015). Characterizing magnetic mineral assemblages of surface sediments from major Asian dust sources and implications for the Chinese loess magnetism. *Earth Planets and Space*, 67, 1-17.

Liu, W., Huang, Y., (2005). Compound specific D/H ratios and molecular distributions of higher plant leaf waxes as novel paleoenvironmental indicators in the Chinese Loess Plateau. *Organic Geochemistry*, 36, 851-860.

Liu, Y., Sun, L., Zhou, X., Luo, Y., Huang, W., Yang, C., Wang, Y., Huang, T. (2014). A 1400-year terrigenous dust record on a coral island in South China Sea. *Scientific Reports*, 4, 4994.

Liu, Z., Colin, C., Huang, W., Le, K.P., Tong, S., Chen, Z., Trentesaux, A. (2007). Climatic and tectonic controls on weathering in south China and Indochina Peninsula: Clay mineralogical and geochemical investigations from the Pearl, Red, and Mekong drainage basins. *Geochemistry, Geophysics, Geosystems*, 8, 1-18.

Liu, Z., Stattegger, K. (2014). South China Sea fluvial sediments: an introduction preface. *Journal of Asian Earth Sciences*, 79, 507-508.

Liu, Z., Zhao, Y., Colin, C., Stattegger, K., Wiesner, M.G., Huh, C.A., Zhang, Y., Li, X., Sompongchaiyakul, P., You, C.F. (2016). Source-to-sink transport processes of fluvial sediments in the South China Sea. *Earth-Science Reviews*, 153, 238-273.

Lu, Z., Gan, J., Dai, M., Zhao, X., Hui, C.R. (20200. Nutrient transport and dynamics in the South China Sea: A modeling study. *Progress in Oceanography*, 102308.

Luo, P., Peng, P., Lü, H., Zheng, Z., Wang, X. (2012). Latitudinal variations of CPI values of long-chain *n*-alkanes in surface soils: Evidence for CPI as a proxy of aridity. *Science China Earth Sciences*, 55, 1134-1146.

Ma, W., Chai, F., Xiu, P., Xue, H., Tian, J. (2013). Modeling the long-term variability of phytoplankton functional groups and primary productivity in the South China Sea. *Journal of Oceanography*, 69, 527-544.

Ma, W., Xiu, P., Chai, F., Li, H. (2019). Seasonal variability of the carbon export in the central South China Sea. *Ocean Dynamics*, 69, 955-966.

Martínez-García, A., Sigman, D.M., Ren, H., Anderson, R.F., Straub, M., Hodell, D.A., Jaccard, S.L., Eglinton, T.I., Haug, G.H. (2014). Iron fertilization of the Subantarctic Ocean during the last ice age. *Science*, 343, 1347-1350.

Mcgee, D., Winckler, G., Borunda, A., Serno, S., Anderson, R.F., Recasens, C., Bory, A., Gaiero, D., Jaccard, S.L., Kaplan, M. (2016). Tracking eolian dust with helium and thorium: Impacts of grain size and provenance. *Geochimica et Cosmochimica Acta*, 175, 47-67.

Ning, X., Chai, F., Xue, H., Cai, Y., Liu, C., Zhu, G., Shi, J. (2005). Physical-biological oceanographic coupling influencing phytoplankton and primary production in the South China Sea. Journal of Geophysical Research Oceans 110, 215-255.

Ohkouchi, N., Kawamura, K., Kawahata, H., Taira, A. (1997). Latitudinal distributions of terrestrial biomarkers in the sediments from the Central Pacific. *Geochimica et Cosmochimica Acta*, 61, 1911-1918.

Pelejero, C. (2003). Terrigenous *n*-alkane input in the South China Sea: high-resolution records and surface sediments. *Chemical Geology*, 200, 89-103.

Pettke, T., Halliday, A.N., Hall, C.M., Rea, D.K., 2000. Dust production and deposition in Asia and the north Pacific Ocean over the past 12 Myr. *Earth and Planetary Science Letters* 178, 397-413.

Priyadarshani, W., Ran, L., Wiesner, M.G., Chen, J., Ling, Z., Yu, S., Ye, Y. (2019). Seasonal and interannual variability of coccolithophore flux in the northern South China Sea. *Deep Sea Research Part I: Oceanographic Research Papers*, 145, 13-30.

Qu, T., (2001). Role of ocean dynamics in determining the mean seasonal cycle of the South China Sea surface temperature. *Journal of Geophysical Research: Oceans*, 106, 6943-6955.

Rao, Z.G., Zhu, Z.Y., Jia, G.D., Henderson, A.C.G., Xue, Q., Wang, S.P. (2009). Compound specific δD values of long chain *n*-alkanes derived from terrestrial higher plants are indicative of the δD of meteoric waters:

evidence from surface soils in eastern China. *Organic Geochemistry*, 40, 922-930.

Ren, H., Sigman, D.M., Martínez-García, A., Anderson, R.F., Chen, M.T., Ravelo, A.C., Straub, M., Wong, G.T. and Haug, G.H., (2017). Impact of glacial/interglacial sea level change on the ocean nitrogen cycle. *Proceedings of the National Academy of Sciences*, 114(33), 6759-6766.

Schefuß, E., Ratmeyer, V., Stuut, J.B.W., Jansen, J.H.F., Sinninghe Damsté, J.S. (2003). Carbon isotope analyses of *n*-alkanes in dust from the lower atmosphere over the central eastern Atlantic. *Geochimica et Cosmochimica Acta*, 67, 1757-1767.

Shen, C., Zhao, H., Chen, F. and Xiao, H., (2020). The Distribution of Aerosols and Their Impacts on Chlorophyll-a Distribution in the South China Sea. *Journal of Geophysical Research: Biogeosciences*, *125*(6).

Shiau, L.J., Yu, P.S., Wei, K.Y., Yamamoto, M., Lee, T.Q., Yu, E.F., Fang, T.H. and Chen, M.T., (2008). Sea Surface Temperature, Productivity, and Terrestrial Flux Variations of the Southeastern South China Sea over the Past 800000 Years (IMAGES MD972142). *Terrestrial, Atmospheric & Oceanic Sciences*, *19*(4).

Still, C.J., Berry, J.A., Collatz, G.J., Defries, R.S. (2009). ISLSCP II C4 Vegetation Percentage. ORNL Distributed Active Archive Center, Oak Ridge, Tennessee, USA.

Sun, Y., Chen, Z., Xu, S., Cai, P. (2005). Stable carbon and hydrogen isotopic fractionation of individual n -alkanes accompanying biodegradation: evidence from a group of progressively biodegraded oils. *Organic Geochemistry*, 36, 225-238.

Tagliabue, A., Bowie, A.R., Boyd, P.W., Buck, K.N., Johnson, K.S., Saito, M.A. (2017). The integral role of iron in ocean biogeochemistry. *Nature*, 543, 51-59.

Tang, D.-L., Ni, I.-H., Kester, D.R., Müller-Karger, F.E. (1999). Remote sensing observations of winter phytoplankton blooms southwest of the Luzon Strait in the South China Sea. *Marine Ecology Progress Series*, 191, 43-51.

Tan, S.C.; Shi, G.Y.; Shi, J. H. (2011). Correlation of Asian dust with chlorophyll and primary productivity in coastal seas of China during the period 1997 to 2008. *Journal of Geophysical Research*, 116, G02029.

Tan, S.C.; Shi, G. Y. (2012). The relationship between satellite-derived primary production and vertical mixing and atmospheric inputs in the Yellow Sea cold water mass. *Continental Shelf Research*, 48,138–145.

Thomas, E.K., Clemens, S.C., Prell, W.L., Herbert, T.D., Huang, Y., Liu, Z., Sinninghe Damste, J.S., Sun, Y., Wen, X. (2014). Temperature and leaf wax 2H records demonstrate seasonal and regional controls on Asian

Formatted: Indent: Left: 0 cm, Hanging: 2 ch, First line: -2 ch

monsoon proxies. *Geology*, 42, 1075-1078.

Tian, J., Wang, P., Chen, R., Cheng, X. (2005). Quaternary upper ocean thermal gradient variations in the South China Sea: Implications for east Asian monsoon climate. *Paleoceanography*, 20, 1-8.

Thunell, R. C., Q. Miao, S. E. Calvert, and T. F. Pedersen, (1992). Glacial-Holocene biogenic sedimentation patterns in the South China Sea: Productivity variations and surface water *p*CO2. *Paleoceanography*, **7**, 143-162.

Uematsu, M., Duce, R.A., Prospero, J.M., Chen, L., Merrill, J.T., Mcdonald, R.L. (1983). Transport of mineral aerosol from Asia Over the North Pacific Ocean. *Journal of Geophysical Research Oceans*, 88, 5343-5352.

Wang, S.H.; Hsu, N.C.; Tsay, S.C.; Lin, N.H.; Sayer, A.M.; Huang, S.J.; Lau, W.K. M. (2012). Can Asian dust trigger phytoplankton blooms in the oligotrophic northern South China Sea? Geophysical Research Letters, 39, L05811.

Wong, G.T., Tseng, C.-M., Wen, L.-S., Chung, S.-W. (2007). Nutrient dynamics and N-anomaly at the SEATS station. *Deep Sea Research Part II: Topical Studies in Oceanography*, 54, 1528-1545.

Xu, W., Yan, W., Chen, Z., Chen, H., Huang, W., Lin, T. (2014). Organic matters and lipid biomarkers in surface sediments from the northern South China Sea: Origins and transport. *Journal of Earth Science*, 25, 189-196.

Yang, H., Pancost, R.D., Dang, X., Zhou, X., Evershed, R.P., Xiao, G., Tang, C., Gao, L., Guo, Z., Xie, S. (2014). Correlations between microbial tetraether lipids and environmental variables in Chinese soils: Optimizing the paleo-reconstructions in semi-arid and arid regions. *Geochimica et Cosmochimica Acta*, 126, 49-69.

Yang, Y., Gao, C., Dang, X.Y., Ruan, X.Y., Lü, X.X., Xie, S.C., Li, X.J., Yao, Y.J., Yang, H. (2018). Assessing hydroxylated isoprenoid GDGTs as a paleothermometer for the tropical South China Sea. Organic Geochemistry, 115, 156-165.

Yang, Y., Ruan, X., Gao, C., Lü, X.X., Yang, H., Li, X., Yao, Y., Pearson, A. and Xie, S., (2020). Assessing the applicability of the long-chain diol (LDI) temperature proxy in the high-temperature South China Sea. *Organic Geochemistry,* 104017.

Zhang, J., Li, H., Xuan, J., Wu, Z., Yang, Z., Wiesner, M.G., Chen, J. (2019). Enhancement of mesopelagic sinking particle fluxes due to upwelling, aerosol deposition, and monsoonal influences in the northwestern South China Sea. *Journal of Geophysical Research: Oceans*, 124, 99-112.

Zhang, R., Chen, M., Yang, Q., Lin, Y., Mao, H., Qiu, Y., Tong, J., Lv, E., Yang, Z., Yang, W. (2015). Physical-biological coupling of N2 fixation in the northwestern S outh C hina Sea coastal upwelling during summer.

546 *Limnology and Oceanography*, 60, 1411-1425.
547
548

Figure Captions

Fig. 1 Distribution of samples used in this study: a) new surface sediment analyses from the South China Sea (red dots); b) surface soil samples previously reported by Rao et al. (2009) and Luo et al. (2012) in the Chinese mainland. The frequency histograms show the geographical distribution of the hydrogen isotopic composition of the C_{31} *n*-alkane in : 1) northeastern China (purple squares, Rao et al., 2009); 2) the shallow and central SCS (red circles, this study) and; 3) the Loess Plateau and Gobi deserts (blue circles, this study). The sequential color gradient (from red to blue) represents heavy to light hydrogen isotope values.

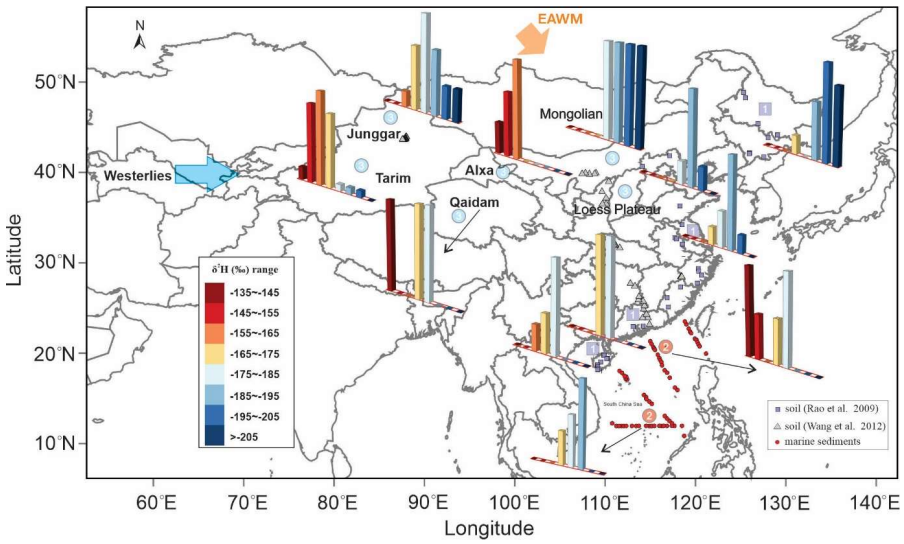

Fig. 2. Water depth distribution of molecular and elemental parameters measured in SCS surface sediments. Marked changes are notable at water depths below 4000 m. a) C/N ratio, b-c) Concentrations of *n*-alkanes and CPI values, d) Concentrations of long chain diols, e-h) Odd (C_{29} and C_{31}) and even (C_{30} and C_{32}) chains hydrogen and carbon alkane isotopes.

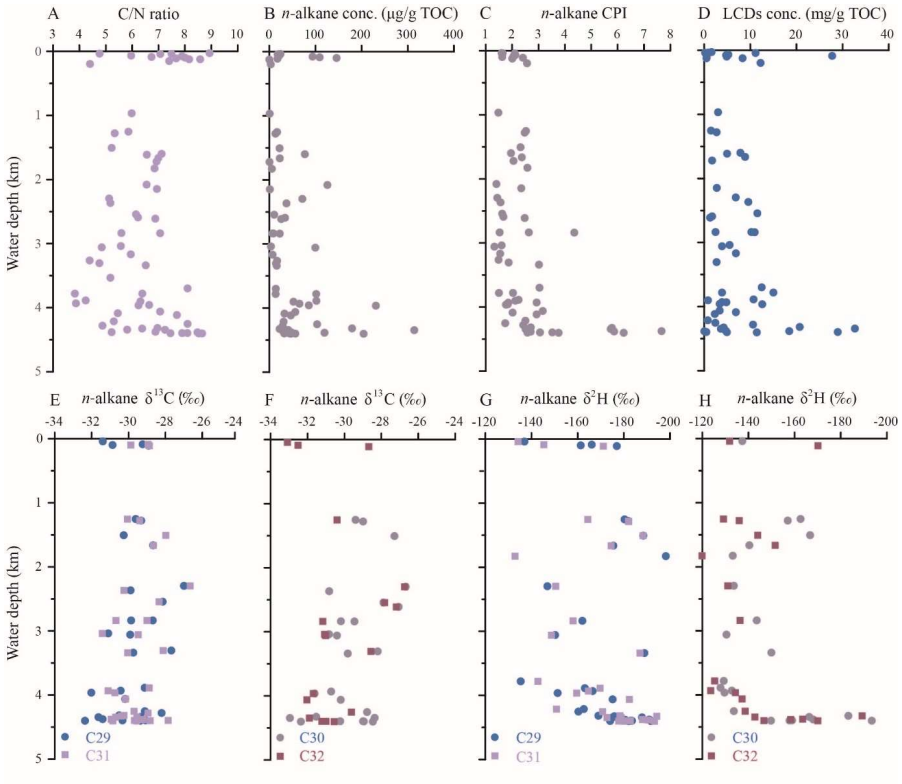

Fig. 3 Spatial distribution of molecular and elemental parameters from the northern to the central basin of the SCS. Distinct values (e.g. high *n*-alkane concentrations, high CPI, isotopically light) are highlighted in the central basin. a-b) Concentrations of n-alkane and long chain diols, c) *n*-alkane CPI value, d) C/N ratio, e-f) carbon and hydrogen isotopes of C_{31} *n*-alkane. The shaded circle roughly show the deep basin with water depth deeper than 2400m.

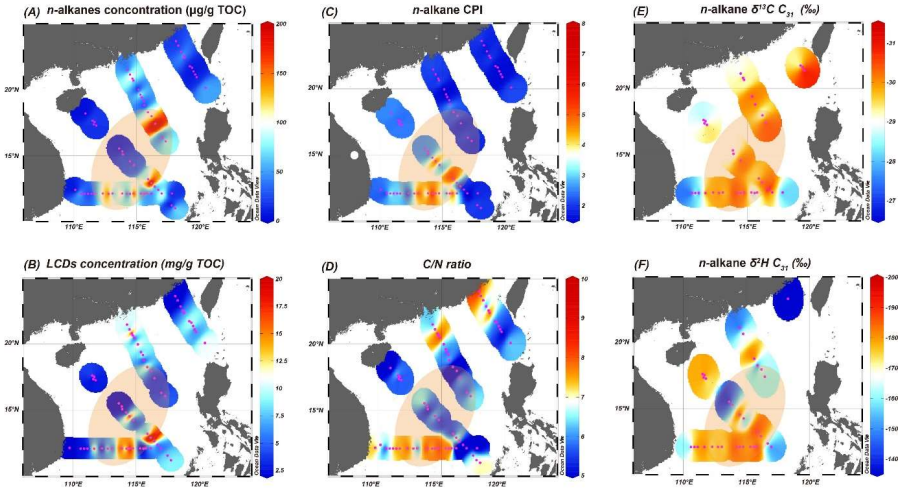

Formatted: Font: Italic

Fig. 4 Latitudinal gradients for Sr-Nd isotopes, CPI values and hydrogen isotopes of *n*-alkanes. These parameters are used to infer the source of dust which has been long-range transported to the deep, central basin of the SCS. A) Correlation between εNd and $^{87}Sr/^{86}Sr$ of SCS surface sediments, modified from Liu et al. (2014). Shaded areas show potential sources for material in the central basin. Data of the Pearl, Red and Mekong rivers from Liu et al. (2007); northern Pacific ocean dust samples are from Pettke et al. (2000). Luzon Arc and Luzon Island samples are from Defant et al. (1990), Philippine Sea samples are from Jiang et al. (2013), Loess samples are from Chen et al. (2007). B) Sr-Nd isotopic compositions of ancient dust falls in North Pacific, and SCS central basin, together with the mixing curve between the <5 μm silicate fractions of the Chinese deserts (Chen et al., 2007) and the volcanic end-member used in Biscaye et al. (1997). The grey dashed lines means the mixing fraction based on end member B and C C), the variation of the CPI values of the *n*-alkanes of the surface soils from different latitude in East China reported by Rao et al. (2009). The dashed line in red shows the maximum of CPI values identified in marine sediments of the deepest water in SCS, with the interception with the regression line (red line) showing the potential dust source; D), the variation of the deuterium content in meteoric water (the original data are available at the website of Global Network of Isotopes in Precipitation (GNIP), http://isohis.iaea.org) and in *n*-alkanes of surface soils in East China reported by Rao et al. (2009). The lowermost perpendicular red dashed lines indicate the most depleted δ^2H values of the *n*-alkanes identified in marine sediments of the deepest waters in the SCS. The interception with the regression line (dashed line in blue) shows the general latitude of the potential dust source.

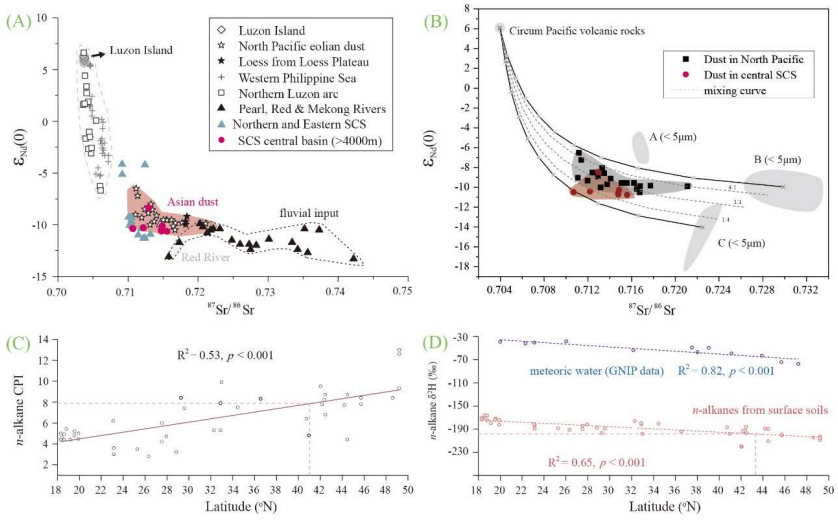

Commented [MOU4]: This appears also red?